The bromodomain protein Bdf3 is sufficient to activate expression of a procyclin gene in bloodstream stage African trypanosomes

Evan J. Kim[1], Ethan L. Goroza[1], Ashley Y. Tan[1], Jolyne J. Lin[1], Kieran C. Saucedo[1], Fuminori Tanizawa[1], Jaclyn E. Smith[2], Danae Schulz[1,*]

[1]Department of Biology, Harvey Mudd College, Claremont, CA
[2]Institute for Genome Sciences, University of Maryland, Baltimore, MD
[*]Corresponding author, dschulz@g.hmc.edu

Abstract

The early branching eukaryotic parasite, *Trypanosoma brucei*, lives extracellularly in the mammalian host, where it expresses variant surface glycoprotein (VSG). Antigenic variation of VSGs allows the parasite to evade the host immune response while in the bloodstream. Upon transition to the tsetse fly vector, the parasite remodels its surface to express procyclin protein from a limited set of *EP* and *GPEET* genes. While the environmental signals that trigger the switch from expressing *VSG* genes to expressing *EP* and *GPEET* genes are known, the molecular mechanism that initiates transcription of the *EP* and *GPEET* genes during parasite differentiation to the procyclic stage within the tsetse is not well understood. Previous work has shown that the chromatin interacting bromodomain protein Bdf3 is absent from the pol I promoter of the *EP* locus in bloodstream parasites, but appears there shortly after initiation of differentiation from the bloodstream to the procyclic stage. Here, we show that tethering of Bdf3 to the *EP* promoter using a dCas9-Bdf3 fusion protein and a guide RNA is sufficient to increase transcript levels of *EP1* in bloodstream parasites, where the gene is normally silenced. This result supports the model that Bdf3 appears at the *EP* locus during differentiation to facilitate initiation of transcription, which is consistent with the role for Bdf3 as a transcriptional activator in other systems. Understanding gene regulatory mechanisms in this early branching eukaryote may help build a more complete picture for the conserved and unique features of gene regulatory proteins across diverse biological systems.

Importance

The *Trypanosoma brucei* parasite is transmitted to a mammalian host via the tsetse fly vector, where it causes African trypanosomiasis, a fatal disease that causes a severe human and economic burden for people living in in areas of sub-Saharan African. While drug treatments have improved for some strains, some infections still require treatment with drugs that have serious side effects. One avenue for drug development is to try and manipulate the lifecycle of the parasite to make it poorly adapted to the mammalian host. However, this requires detailed knowledge of the mechanisms by which parasites regulate their genes as they progress through the lifecycle. Here, we show that the DNA interacting bromodomain protein Bdf3 may be a key driver for turning on insect-specific genes that code for insect-stage surface proteins. This finding could aid in the

development of lifecycle manipulating drugs, and shed light on how gene regulatory mechanisms evolved.

Introduction

Numerous parasites transition between hosts as part of their natural life cycle. Because host environments can differ dramatically with respect to temperature, pH, and nutrient availability, parasites that transition between hosts must evolve systems to adapt to differing environments. One such parasite is the African trypanosome, *Trypanosoma brucei*. *T. brucei spp.* are unicellular, eukaryotic protozoan parasites that infect humans and ungulates and cause Human and Animal African Trypanosomiasis disease. African trypanosomiasis is usually fatal, and imposes a severe human and economic burden for people living in Sub-Saharan Africa, where the disease is endemic (1, 2). *T. brucei* cycle between a tsetse fly vector and the bloodstream of a mammalian host, where they live extracellularly. Compared to the tsetse, the bloodstream environment of the mammalian host is warmer and glucose rich, and the parasite must contend with a robust antibody response mounted by the host immune system. The parasite has evolved to live in the mammalian bloodstream by antigenically varying the proteins on its surface, which are coded for by a large repertoire of Variant Surface Glycloprotein (*VSG*) genes (3). Antigenic variation of VSG surface proteins allows bloodstream parasites to successfully evade the host antibody response. Upon transition to the fly midgut following a tsetse bloodmeal, the parasites alter their glucose metabolism (4–7) and express a far more limited repertoire of procyclin surface proteins coded by the *GPEET* and *EP* genes (8). GPEET proteins contain a pentapeptide repeat of the GPEET amino acid sequence, while EP proteins contain a dipeptide repeat (8, 9). *GPEET, EP1, EP2,* and *EP3* are all co-expressed within the first few hours after differentiation to the procyclic form. GPEET protein predominates on the parasite surface early in development, and this protein is replaced with EP isoforms later in development within the midgut (10). Since the tsetse lacks an antibody-based immune response, antigenic variation of *VSG* genes is no longer required, and instead the GPEET and EP procyclin proteins shield the parasites from proteases expressed by the tsetse (11). Thus, remodeling of the parasite surface is essential to survive following transition to either the bloodstream or the tsetse environments.

While it has been established that expression of *GPEET* and *EP* genes is transcriptionally and developmentally regulated (12, 13), the molecular mechanism that initiates transcription of these genes following parasite transition to the fly is poorly understood. Unusually for a eukaryote, the *GPEET* and *EP* protein coding genes are transcribed by Pol I (12, 14–16). Because most protein coding genes in *T. brucei* are transcribed by Pol II in polycistronic units with limited transcriptional regulation (reviewed in (17) and recently corroborated with SLAM-seq (18)), the transcriptionally controlled procyclin genes offer a unique opportunity to examine transcriptional regulation in a highly diverged, early branching eukaryote.

Despite the lack of transcriptional control for pol II genes, *T. brucei* parasites do harbor much of the machinery associated with the histone code that is best characterized in model systems such as yeast, worms, and flies (19). This machinery includes numerous post-translational modifications of histone proteins (20) as well as proteins that read, write, and erase those modifications (21–28). One of the best characterized domains found in proteins that act as chromatin readers is the bromodomain, which recognizes acetylated lysines on histone tails and has an established role in gene activation (29–33). In murine models, bromodomain proteins maintain cell identity and help regulate differentiation (34–36).

Bromodomain proteins have also been examined in protozoan parasites, where it has been found that inhibition via small molecules or genetic manipulation results in defects in transcription for *Toxoplasma gondii* (37) and *Leishmania mexicana (38)* as well as developmental blocks in *Trypanosoma cruzi* (39, 40) and *Plasmodium falciparum* (41, 42). Small molecule inhibition of bromodomain proteins causes defects in egg development in *Schistosoma japonicum (43)*. In *T. brucei*, bromodomain proteins are also involved in differentiation processes, both in bloodstream (25) and in procyclic (44) stages. *T. brucei* contains 7 proteins with bromodomains identified through homology (21, 26, 45). Bdf1-6 bind transcription start sites in bloodstream parasites (21, 25, 26), while Bdf7 localizes to transcription termination regions (26). Staneva et al. classified Bdf1, Bdf3, and Bdf4 as Class I transcription start region associated factors because of the sharp, high peaks observed in ChIP-seq experiments using antibodies against Bdf1, Bdf3, and Bdf4. Based on their genomic distribution, the authors hypothesized that Bdf1, Bdf3, and Bdf4 were likely to be involved in transcription initiation (26). Bdf2, Bdf5, and Bdf6 showed broader distributions, and thus were classified as Class II transcription start region associated factors. Bdf2, Bdf5, and Bdf6 were hypothesized to be involved in transcriptional elongation based on this distribution (26). Based on their genomic localization at pol II transcription start sites and association with transcriptional activation, we hypothesized that bromodomain proteins in *T. brucei* might also be important for initiating transcription of pol I driven procyclin genes that are transcriptionally activated as parasites transition from the bloodstream to the insect stage.

Using CUT&RUN (46), we followed the genomic localization of the bromodomain protein Bdf3 in pleomorphic parasites induced to differentiate from the bloodstream to the procyclic stage via treatment with cis-aconitate and incubation at 27ºC (47). We found that both the *EP* locus and the *GPEET* locus lacked genomic occupancy of Bdf3 in bloodstream parasites. 3 hours after differentiation was induced, we observed *de novo* occupancy of Bdf3 at both the *EP* locus and the *GPEET* locus. Indeed, these were the only loci analyzed where Bdf3 was consistently absent from a genomic site in bloodstream parasites but present following induction of differentiation (48). While the presence of Bdf3 at the *EP* and *GPEET* loci implicates the protein as contributing to initiation of transcription at that locus, its mere presence does not definitively prove its ability to increase transcript levels of procyclin genes. We thus set out to test whether Bdf3 was sufficient to increase transcript levels at the *EP1* locus in bloodstream parasites,

133 where the locus should normally be silenced. We engineered a tethering system inspired
134 by CRISPR activation-based systems developed for other organisms (49, 50) and
135 introduced it into a previously validated reporter system for *EP1* transcript levels (51).
136 This system allowed us to artificially drag Bdf3 to the *EP1* locus in bloodstream parasites,
137 where *EP1* is normally silenced. Here, we show that Bdf3 is sufficient to increase
138 transcript levels of *EP1* under these conditions. This system can be used as a platform to
139 study transcriptional activation for a host of other putative activators.
140

141 ## Results

142

143 ### The dCas9-Bdf3 fusion protein is inducibly expressed in *Trypanosoma brucei*

144

145 Previous work in our lab showed that Bdf3 is absent from the *EP1* promoter in
146 bloodstream parasites (48). After treatment with cis-aconitate and incubation at 27ºC to
147 induce differentiation to the procyclic form, Bdf3 localizes to the *EP* locus at 3 hours post
148 induction and remains there until differentiation is completed at 72h post-induction (48).
149 However, whether Bdf3 occupancy at the *EP1* locus is sufficient to increase transcript
150 levels of the *EP1* gene is unknown. In order to test whether Bdf3 is sufficient to induce
151 expression of *EP1* in bloodstream parasites, we cloned a construct that would allow us to
152 artificially recruit Bdf3 to the *EP1* locus in *EP1/GFP* reporter bloodstream parasites (51).
153 To do this, we fused the entire Bdf3 open reading frame to a catalytically dead version of
154 the Cas9 protein (dCas9) using a flexible GS linker (52). The dCas9 protein is recruited
155 to a specific genomic locus using a guide RNA, but two mutations in the active site prevent
156 dCas9 from creating a double strand break at that location (49, 53). In model systems,
157 fusion of dCas9 to transcriptional activation domains (CRISPR activation) or
158 transcriptional inhibition domains (CRISPR inhibition) and targeting of these fusion
159 proteins to a gene promoter using a guide RNA modulates transcription for the target
160 gene (49, 50). CRISPR activation and CRISPR inhbition systems have been successfully
161 adapted in mammalian cells, plants (54), and in the protozoan parasite *Plasmodium*
162 *falciparum* (55). Excellent work adapting CRISPR-Cas9 systems for genome editing in *T.*
163 *brucei* (56–58) allowed us to take advantage of previously built constructs to set up the
164 CRISPR activation system. To our knowledge, we are the first to adapt a dCas9-based
165 CRISPR-activation system to *T. brucei*.
166

167 To address whether Bdf3 can increase transcript levels at a silent locus, our FLAG tagged
168 dCas9-Bdf3 fusion construct was cloned into a vector that allows inducible expression
169 using the tetracycline-on system (tet-on) (Fig. 1A, top) (59). The construct was stably
170 integrated into the genome using homology to the rDNA locus. An additional FLAG tagged
171 dCas9 construct was integrated to use as a control. Treatment for 1 day or 2 days with
172 doxycycline (dox) showed inducible expression of both the dCas9-Bdf3 fusion protein and
173 the dCas9 protein in transfected parasites, with both proteins appearing at the expected
174 size (Fig.1B, Fig. 1C). We did not observe background expression of dCas9-Bdf3 in the -
175 Dox condition for any of the three clones (Fig. 1B). We observed a robust expression
176 increase in dCas9 protein levels after doxycycline treatment, although a faint band was

177 observed in both clones in uninduced samples (-dox). Thus, we proceeded with clone 1.
178 As an additional control, we cloned the Bdf3 open reading frame into the same vector that
179 was used for both dCas9-Bdf3 and dCas9 alone and tested inducible expression by
180 western blot (Fig. 1D). We observed the lowest level of background expression in Clone
181 2, as evidenced by undetectable protein in the -Dox condition, and so further experiments
182 continued with this clone. Once inducible expression was verified for both the dCas9-Bdf3
183 strain and the dCas9-alone strain, we transfected both strains with guide RNAs targeted
184 to either the *EP1* promoter or a locus unrelated to differentiation. We chose the *NEO* locus
185 to use as the unrelated control. The *NEO* gene was previously used to select for
186 integration of the T7 polymerase and tet repressor (59), which is present in the
187 background of the *EP1/GFP* reporter strain. Guide RNA constructs were designed to
188 target the *EP1* promoter (12, 14, 16, 60) or the *NEO* gene using the Eukaryotic Pathogen
189 CRISPR guide RNA/DNA Design Tool (61). Tet/dox inducible guide RNA constructs were
190 stably integrated into the trypanosome genome using selection with phleomycin (Fig. 1A),
191 as in (56).
192

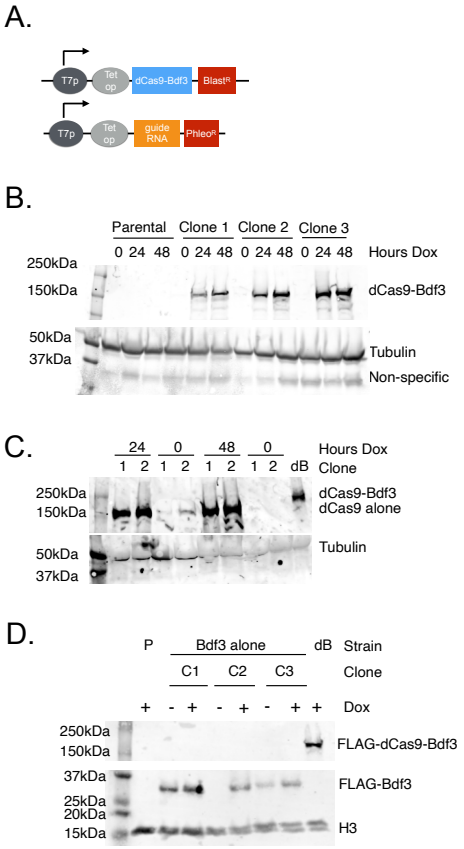

Figure 1. The dCas9-Bdf3 fusion protein and the dCas9 protein are inducibly expressed. (A) Schematic of constructs integrated into the *T. brucei* genome in order to inducibly express the dCas9-Bdf3 fusion protein and the guide RNAs. T7p, T7 promoter, Tet op, tetracycline operator Blast^R, *BSD* gene to generate resistance to blasticidin. Phleo^R, *BLE* gene encoding resistance to phleomycin. Both constructs are targeted to the rDNA locus. (B) Western blot of *T. brucei* extracts transfected with the dCas9-Bdf3 fusion construct and harvested at the indicated timepoints following treatment with 1μg/ml dox. 3 independent clones were analyzed along with a parental control that was not transfected with the dCas9-Bdf3 construct (labeled Parental). Blots were probed with anti-FLAG to detect dCas9-Bdf3 and anti-tubulin to detect tubulin protein. (C) Western blot of *T. brucei* extracts transfected with the dCas9 alone construct and harvested at the indicated timepoints following treatment with 1μg/ml dox. 2 independent clones were analyzed and an extract containing a dCas9-Bdf3 construct was used as a positive control (labeled dB). Blots were probed with anti-FLAG to detect dCas9 and dCas9-Bdf3 and anti-tubulin to detect tubulin protein as a loading control. (D) Western blot of *T. brucei* extracts transfected with the Bdf3 construct and harvested after 48h of treatment with 1μg/ml dox. – indicates untreated samples. 3 independent clones were analyzed (labeled C1, C2, and C3) along with a parental control that was not transfected with the Bdf3 construct. An extract containing a dCas9-Bdf3 construct was used as a positive control (labeled dB). Blots were probed with anti-FLAG to detect Bdf3 and dCas9-Bdf3 and anti-H3 to detect histone H3 as a loading control.

The bromodomain protein Bdf3 is sufficient to increase transcript levels of *EP1/GFP* when targeted to the *EP1* locus

To ascertain whether Bdf3 is sufficient to increase transcript levels of *EP1/GFP* bloodstream parasites where it should not be highly expressed, we measured *EP1/GFP* levels by flow cytometry in *EP1/GFP* reporter parasites harboring either *EP1* guides or *NEO* guides in both dCas9-Bdf3 strains and dCas9 alone strains. 3 different clones were chosen to analyze for each guide RNA tested, and dox was used to induce expression of both the guide RNA and either the dCas9-Bdf3 fusion protein, or the dCas9 alone protein. Flow cytometry measurements were taken after 48h and 72h of dox treatment. For most clones, additional biological replicates were analyzed, except in the case where a clone was inadvertently lost. For each sample, the mean GFP fluorescence intensity was obtained for the +Dox treatment where dCas9-Bdf3, dCas9 alone and the guide RNA were induced, and also the uninduced -Dox treatment used as the control. The fold change in mean GFP fluorescence intensity for the +Dox versus the -Dox samples was computed and is shown in Fig. 2. We found that there was a significant increase in +Dox/-Dox fold changes for mean GFP fluorescence intensity at both time points in dCas9-Bdf3 parasites targeted to the *EP1* locus using two different guide RNAs (dCas9-Bdf3 EP1-1 and dCas9-Bdf3 EP1-3) when compared to control dCas9-Bdf3 parasites targeted to the *NEO* locus (dCas9-Bdf3 NEO-1) (Fig. 2, S1 Fig., S1 Table, S2 Table). This result indicates that the increase in *EP1/GFP* expression occurs only when the fusion protein is targeted to the *EP1* locus, and is thus locus dependent. We also found that there was a significant increase in +Dox/-Dox fold changes in mean GFP fluorescence intensity when dCas9-Bdf3 parasites targeted to the *EP1* locus were compared to dCas9 alone parasites targeted to the *EP1* locus at both timepoints, indicating that dCas9 alone is not sufficient to increase *EP1/GFP* and that Bdf3 is also required (Fig. 2, S1 Table, S2 Table). We do not have evidence that overexpression of Bdf3 alone is sufficient to increase transcript levels of *EP1/GFP*, as there was no significant difference in mean GFP fluorescence intensity fold changes for Bdf3 alone parasites compared to dCas9 alone parasites targeted to either *NEO1* or *EP1* (S1 and S2 Tables). Lastly, there is no significant difference in +Dox/-Dox fold changes in dCas9 alone parasites targeted to *EP1* compared to dCas9 alone parasites targeted to the *NEO* locus. We conclude that Bdf3 is sufficient to increase transcript levels of *EP1/GFP* when targeted to the *EP1* locus. Given that Bdf3 appears at the *EP1* locus after differentiation from the bloodstream to the procyclic stage is initiated (48), our data support a model in which Bdf3 facilitates transcription at the *EP1* locus once differentiation has been triggered.

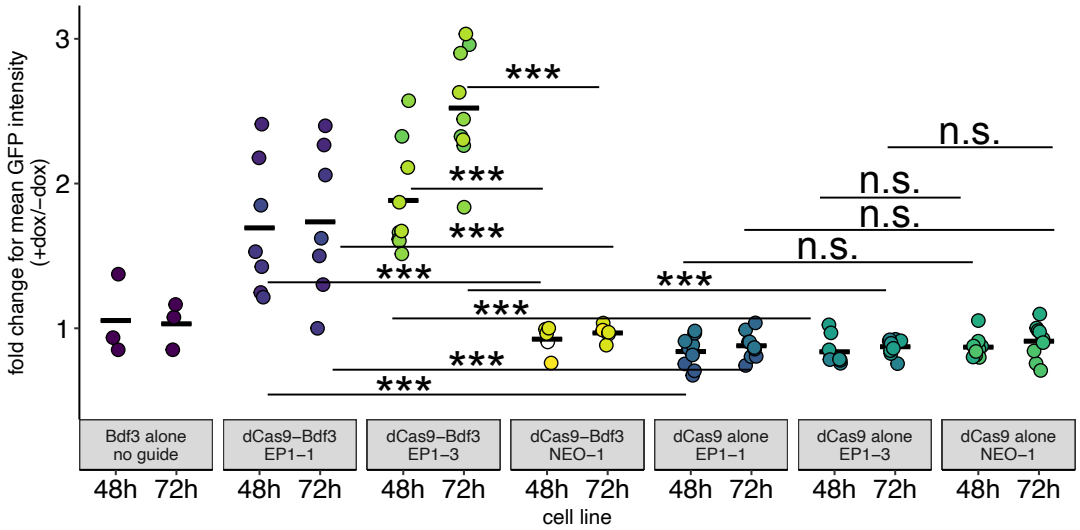

253
254 **Figure 2. dCas9-Bdf3 targeted to the *EP1* locus is sufficient to increase *EP1/GFP* transcript**
255 **levels in bloodstream *T. brucei* parasites.** Quantification of flow cytometry data processed to
256 compute the fold change in mean fluorescence intensity of parasites treated with dox vs untreated
257 parasites. 1μg/ml dox treatment was used to induce expression of dCas9-Bdf3, dCas9 alone,
258 Bdf3 alone and guide RNAs targeted to either the *EP1* locus (EP1-1 and EP1-3 guides) or the
259 *NEO* locus (NEO-1 guide). 3 independent clones were analyzed for each the dCas9-Bdf3 and
260 dCas9 alone strains. Only one clone of Bdf3 alone was analyzed with 3 biological replicates. Dots
261 are color coded such that biological replicates for the same clone are the same color. Data was
262 analyzed using ANOVA followed by a Tukey HSD (Honestly Significant Difference) post-hoc
263 analysis. Two different ANOVA analyses were performed, one for 48h and one for 72h dox
264 treatment. *, $p < 0.05$, **, $p < 0.01$, ***, $p < 0.001$, n.s. not significant. The figure indicates the
265 most relevant statistical comparisons. A full set of p values for each comparison is provided in S1
266 Table and S2 Table.
267
268

Expression of the dCas9-Bdf3 fusion protein targeted to the *EP1* locus causes a mild growth defect

In order to assess whether expression of *EP1/GFP* induced by dCas9-Bdf3 causes a growth defect, we performed growth assays on both *EP1* and *NEO* guide RNA parasites expressing either the dCas9-Bdf3 fusion protein or dCas9 alone. We observed a mild growth defect in dCas9-Bdf3 parasites targeted to *EP1* after 48h of induction, while this growth defect was not observed in any other strain we tested (Fig. 3). We do not think the growth defect is caused solely from the expression of the dCas9-Bdf3 fusion protein because parasites induced to express dCas9-Bdf3 targeted to the *NEO* locus do not exhibit a growth defect.

Multiple researchers have shown that expression of more than one VSG protein can lead to growth defects (62–65), and it's possible that the expression of both *VSG* and *EP1* might cause a similar phenotype. Another possibility relates to the growth arrested nature of stumpy parasites, which are an intermediate stage that occurs when bloodstream parasites grow to high density; these parasites have been shown to pre-express *EP1* prior to transition to the fly (66). While the monomorph strains we used in this experiment do not form a true stumpy intermediate, the increased transcription of *EP1* might cause the parasites to acquire some stumpy-characteristics, causing a reduction in growth. Small molecules that induce expression of *EP1* have also been associated with growth defects (51). A study using a procyclin reporter also found that some compounds that induced procyclin reporter activity also inhibited growth of the parasites (67). Thus, while we do not know the exact mechanism for the observed growth defect in dCas9-Bdf3 parasites targeted to the *EP1* locus, other studies have shown that growth inhibition is often associated with an increase in *EP1* transcript levels.

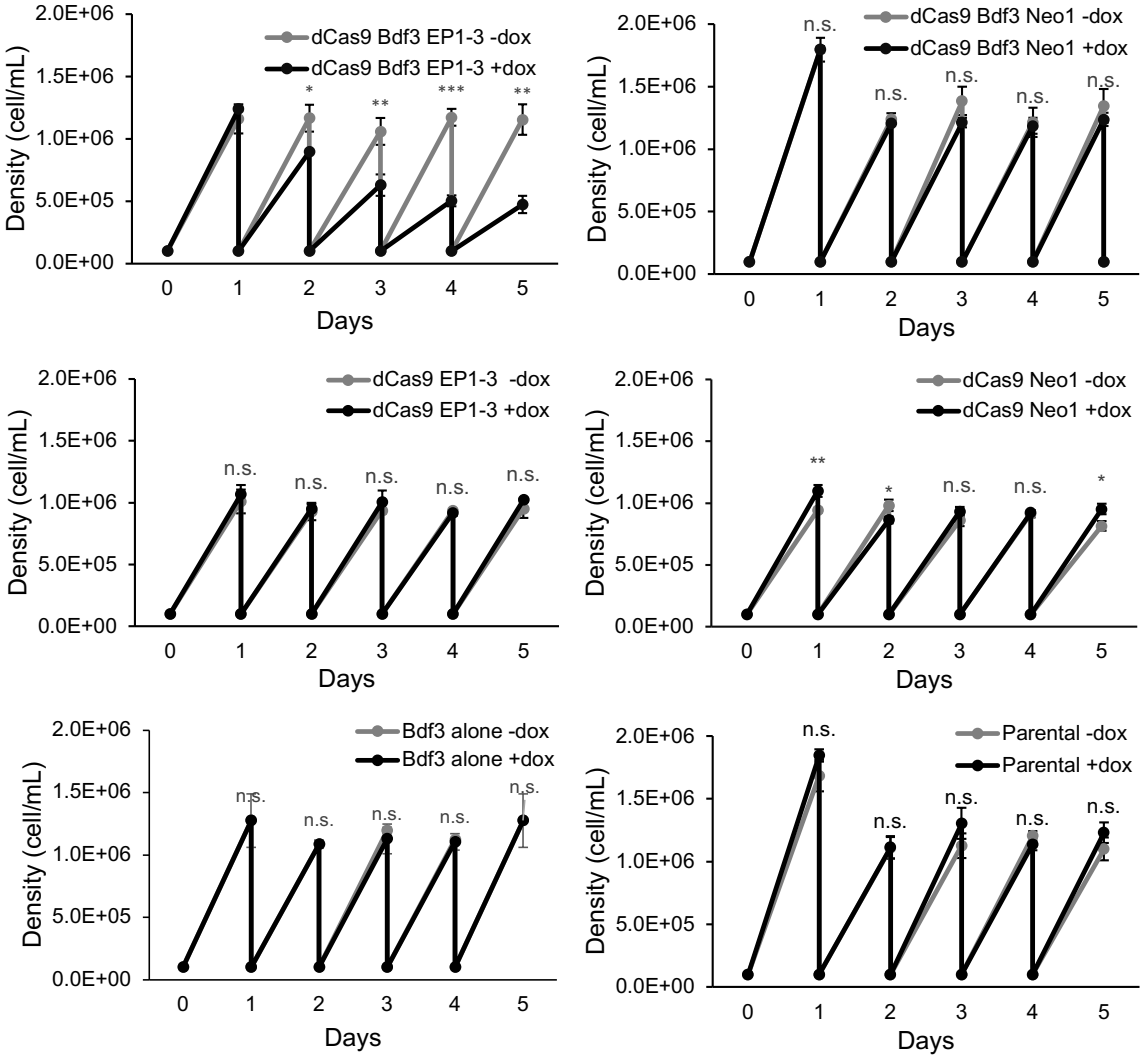

Figure 3. Expression of dCas9-Bdf3 targeted to the *EP1* locus causes a growth defect after induction of dCas9-Bdf3 and the guide RNA. Parasites were seeded at 100,000 cells/ml with or without 1μg/ml dox and grown for 24h before being counted and diluted back to 100,000 cells/ml over the course of 5 days. A Student t-test was used to compared -dox and + dox samples for each parasite strain at each time point. *, $p < 0.05$, **, $p < 0.01$, ***, $p < 0.001$. n.s. not significant.

304 **Transcript levels of *EP1, GPEET, and PAG2* are increased after expression of**
305 **dCas9-Bdf3 targeted to the *EP1* locus.**
306
307 To verify the flow cytometry results, we measured *EP1* transcript levels directly using q-
308 PCR on parasites induced to express dCas9-Bdf3 targeted to the *EP1* locus or to the
309 control *NEO* locus following 3 days of Dox treatment. We found that both *EP1* and *GFP*
310 transcript levels were higher in parasites induced to express dCas9-Bdf3 and a guide
311 RNA targeted to *EP1* compared to uninduced parasites (Fig. 4A). Parasites induced to
312 express dCas9-Bdf3 and a guide RNA targeted to the control *NEO* locus did not show an
313 increase in expression of either *EP1* or *GFP*, as expected (Fig. 4B). In addition,
314 expression of a control gene *SF1* (splicing factor 1) that was not expected to change
315 following induction of dCas9-Bdf3 showed no significant change in expression when
316 dCas9-Bdf3 was targeted to either the *EP1* locus or the *NEO* locus (Fig. 4A, Fig. 4B).
317 Because the promoter sequence for *EP1* and *GPEET* are highly similar, we expected that
318 guide RNAs targeted to the *EP1* promoter may also tether dCas9-Bdf3 to the *GPEET*
319 locus, resulting in an increase in *GPEET* expression when both dCas9-Bdf3 and the guide
320 RNA are induced with dox. This hypothesis was supported by an increase in expression
321 of the *GPEET2* gene following induction of both dCas9-Bdf3 and the *EP1* guide RNA (Fig.
322 4A). No increase in *GPEET2* expression levels was observed in parasites induced to
323 target dCas9-Bdf3 to the *NEO* locus. Given that the *PAG2* gene is found in the same
324 polycistronic unit as *EP1*, we measured the expression levels of *PAG2* following induction
325 of dCas9-Bdf3 targeted to the *EP1* locus. Expression levels of *PAG2* were significantly
326 increased in dCas9-Bdf3 parasites expressing guide RNAs targeted to *EP1* compared to
327 uninduced parasites (Fig. 4A). These changes were not observed when dCas9-Bdf3 was
328 targeted to the control *NEO* locus (Fig. 4B). The observed increase in *EP* and *GPEET*
329 expression in parasites expressing dCas9-Bdf3 targeted to the *EP1* locus are not as large
330 as the changes observed in expression of these genes as parasites are fully
331 differentiating from the bloodstream to the insect stage (51, 68, 69). This observation is
332 consistent with the fact that multiple modes of stabilizing *EP* and *GPEET* transcripts are
333 in play in fully differentiating parasites. Stabilization of *EP* and *GPEET* transcripts has
334 been shown to be mediated through UTR sequences (70–72) and trans-acting factors
335 (73, 74). Environmental factors such as nutrient availability can also influence *GPEET*
336 transcript stability (72, 75). Thus, it is not surprising that transcript levels of *GPEET* and
337 *EP1* observed in dCas9-Bdf3 *EP1* targeted parasites are not as high transcript levels
338 observed in differentiating parasites. Finally, multiple different bromodomain protein
339 complexes have been shown to localize to pol II promoters (26). It is possible that
340 additional transcriptional activators, in addition to Bdf3 and its associated complex
341 members, are required to achieve high transcript levels at the *EP1* promoter or pol I
342 promoters in general.
343
344 Previous work in our lab has showed that treatment of *T. brucei* parasites with either
345 spironolactone or eflornithine causes an increase in expression of *EP1, GFP, and PAG2,*
346 and that these changes are accompanied by other changes in transcript levels that occur
347 as parasites transition from the bloodstream to the insect stage (51). These changes

348 include a decrease in expression of genes that are important in the glycolysis pathway,
349 including *PYK1, HK1, ALD*, and *GIM5B*. We were surprised to see that transcript levels
350 of *HK1, GIM5B and ALD* were slightly decreased in parasites where dCas9-Bdf3 was
351 induced and targeted to the *EP1* locus (Fig. 4A). No significant changes in transcript levels
352 for these genes was observed in parasites where dCas9-Bdf3 was induced and targeted
353 to the control *NEO* locus (Fig. 4B). A silent *VSG* gene (VSG18) was also slightly
354 upregulated, which has also been previously observed in conjunction with changes in
355 *EP1* expression (25). The unexpected decrease in transcript levels for genes associated
356 with glycolysis may indicate that a feedback loop of unknown mechanism may exist in
357 parasites for which *EP1* transcript levels are increased. Increases in transcript levels for
358 *EP1* and *GPEET* have been observed in conjunction with a decrease in transcript levels
359 for glycolysis genes in stumpy parasites that undergo transcriptional pre-adaptation to life
360 in the tsetse (66, 68), so there is precedent for these changes occurring together.
361 However, we did not necessarily expect a differentiation program to initiate following an
362 increase in *EP1* transcript levels, and this phenomenon might be worth exploring in future
363 work. It should also be emphasized that the observed difference in transcript levels for
364 glycolysis genes is quite muted compared to the much more dramatic changes in
365 transcript levels observed in bloodstream parasites induced to differentiate to the
366 procyclic form (68, 69).
367

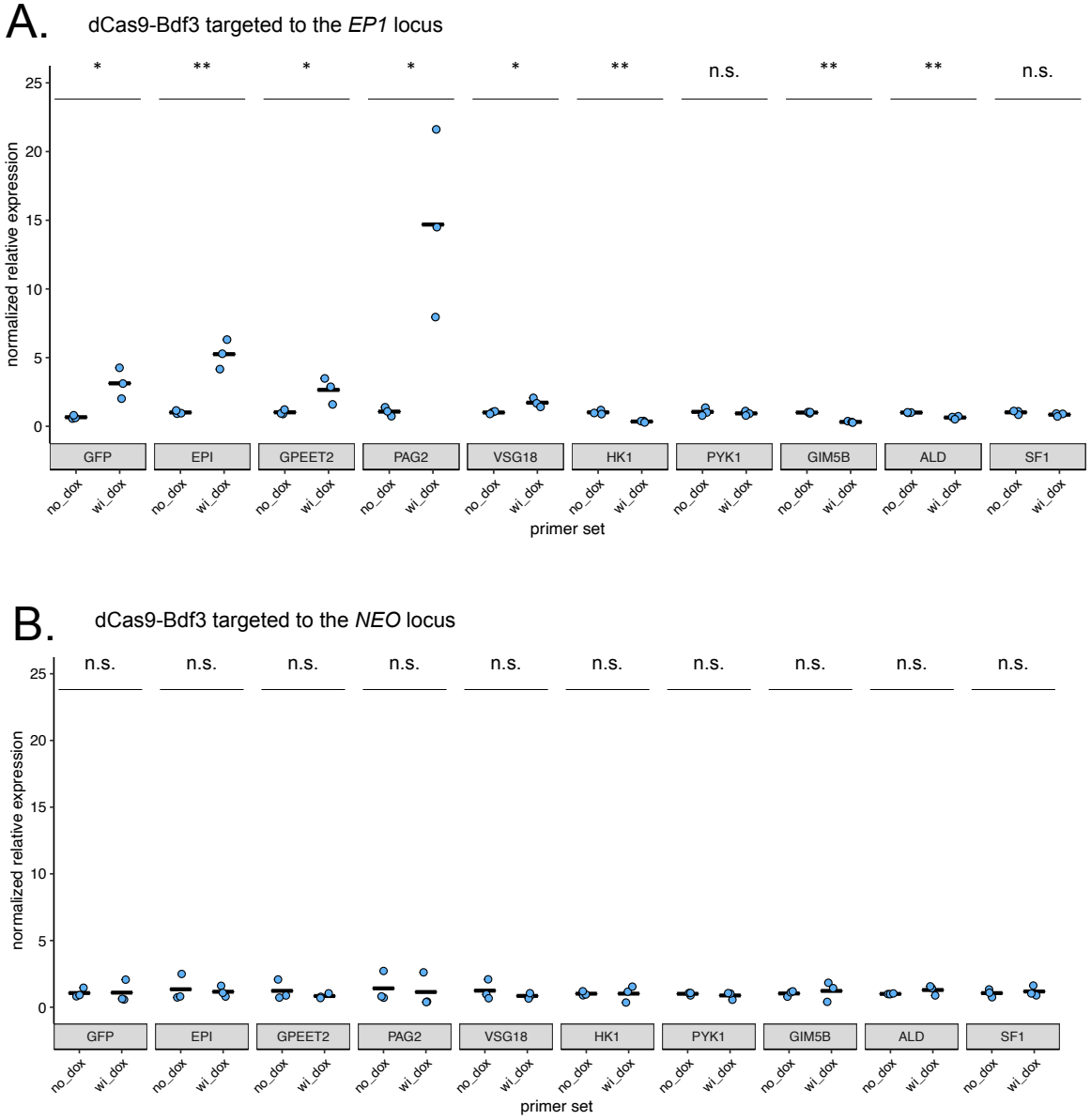

Figure 4. dCas9-Bdf3 targeted to the *EP1* locus results in increased expression of *EP*-related genes. Relative expression of each indicated gene analyzed using quantitative PCR from cDNA generated from RNA extracts of parasites harboring dCas9-Bdf3 targeted to the *EP1* locus (A) or dCas9-Bdf3 targeted to the *NEO* locus (B). Parasites were treated with dox for 72h to induce maximal expression of dCas9-Bdf3 and the guide RNA. Scaling was performed such that the average -Dox value for each gene was set to 1 to allow for easy comparisons between samples. Each dot represents the average of 3 technical replicates and the set of 3 dots for each sample represents 3 biological replicates for 3 independent clones. A Student t-test was performed to compare +Dox samples vs -Dox samples. *, $p < 0.05$, **, $p < 0.01$, ***, $p < 0.001$, n.s. not significant. wi_dox, with dox

383 ## Discussion
384
385 While the role for bromodomain proteins as transcriptional activators in mammalian cells
386 is well established, whether these proteins are important for facilitating transcription
387 initiation in trypanosomes is less clear. Here, we show that the bromodomain protein Bdf3
388 is sufficient to increase transcript levels for a gene that is normally silenced in bloodstream
389 parasites (Fig. 2). Both Bdf3 and a guide RNA targeting the *EP1* promoter are required
390 to observe an increase in *EP1* transcript levels (Fig. 2).
391
392 One thing that remains unclear is whether acetylation at the promoter of the *EP1* locus is
393 required for Bdf3 to increase transcript levels. In many model systems, bromodomains
394 and histone acetylation domains are often found in one protein, allowing both acetylation
395 of histones and reading of that acetylation to be accomplished by the same protein.
396 Examples include p300, CBP, PCAF, and GCN5, among others (76). In *T. brucei*, none
397 of the 7 identified proteins with bromodomains also contain a HAT domain, but there are
398 3 other identified *T. brucei* proteins with HAT domains (22). Elegant experiments using
399 immunoprecipitation combined with mass spectrometry have shown that Bdf3 complexes
400 with both Bdf5 and Hat2 (26). Depletion of Hat2 in *T. brucei* alters the site of transcription
401 initiation in *T. brucei* (77). Hat2 has been shown to acetylate H4K10 (22, 77), which is
402 found at pol II promoters (21), and recruitment of Hat2 by Bdf3 might result in this same
403 acetylation at the *EP1* promoter in our experiments. Bdf3 has also been shown to be
404 important for deposition of H2A.Z at transcription start sites for pol II promoters (21, 78).
405 However to our knowledge, aside from Bdf3 (48), it remains unclear whether the histone
406 modifications and proteins observed at pol II promoters are also found at the pol I
407 promoters of *EP* and *GPEET* as parasites differentiate from the bloodstream stage to
408 stumpy forms and then to procyclic stages. This is an interesting area for future study.
409 Our favored model is that increases in H4K10ac at the *EP1* promoter may drive
410 recruitment of Bdf3 that is observed in differentiating parasites. Resynthesis of an
411 H4K10ac-specific antibody would provide the tools to interrogate this question.
412
413 To our knowledge, we are the first group to engineer a CRISPR activation-type system in
414 *T. brucei*. It remains unclear whether the tool could be easily adapted to overexpress
415 proteins of interest. Because most pol II genes are expressed polycistronicly from
416 transcription start sites, designing a guide to a specific transcription start site and
417 increasing transcription at that site would be expected to increase transcription of multiple
418 genes simultaneously. In addition, because most transcript levels are regulated post-
419 transcriptionally through 5' and 3' UTRs (79, 80), pseudouridination (81), lncRNAs (82),
420 and alternative polyadenylation (83), increasing transcription at the relevant start site
421 may not have any effect on transcript levels for the gene of interest if these other modes
422 of regulation dominate. If a construct containing the gene of interest is placed downstream
423 of a unique promoter and incorporated exogenously, overexpression may be achievable
424 through expression of the dCas9-Bdf3 fusion in conjunction with a guide RNA targeted to
425 the promoter. However, the already existing tet inducible system (59) may offer the same
426 advantages with less engineering.

One outstanding question that should be addressed in future work is whether Bdf3 is capable of inducing expression from any promoter, or whether there is something unique about the *EP1* locus. This issue has been difficult to address because only a very limited number of genes are transcriptionally regulated in different life cycle stages. In order to rigorously address this question, the promoter in question would ideally be silent in at least one life cycle stage. The promoters upstream of silent *VSG* genes are one example of a region that is silenced in bloodstream parasites, but because the expression site promoters share a great deal of homology, trying to target dCas9-Bdf3 to these promoters may be difficult because the protein would be diluted among many different sites. Another way to address this could be to design a guide RNA to an alternate exogenously introduced promoter. Many *T. brucei* expression constructs utilize either the *GPEET* or the *EP* promoter to drive expression, but utilization of the rRNA promoter is also common. Designing guide RNAs targeting the rRNA promoter and examining the effect on transcript levels of the adjacent gene would address whether Bdf3 is sufficient to increase transcript levels at multiple promoter types. However, because the rRNA promoter is strong and constitutively active in bloodstream parasites, it is possible that the addition of dCas9-Bdf3 would not boost the signal significantly if it is already 'maxed out', so to speak. Thus, a negative result for this experiment may be difficult to interpret. Because *NEO* is controlled by readthrough transcription in our trypanosome system, we did not attempt to control *NEO* expression using guide RNAs. Guide RNAs targeted to the *NEO* gene body were simply used as a sink for dCas9-Bdf3 to avoid untargeted interactions with other regions of the genome, something that is a known issue in the absence of a decoy or irrelevant guide RNA (84, 85).

Another useful feature of the engineered dCas9-Bdf3 system is that mutation analyses can now be used to determine what features of the protein are necessary to achieve the increased transcript levels observed when Bdf3 is targeted to the *EP1* locus. Mutation of a conserved tyrosine and asparagine (86, 87) in the bromodomain would allow interrogation for the requirement to bind acetylated histones. Truncations might also assist in determining what portions of the protein are necessary to recruit Hat2 and Bdf5, if any. Finally, Bdf3 is one of six trypanosome bromodomain proteins shown to localize to transcription start sites (21, 25, 26). The dCas9 fusion system that we have engineered can be used to ascertain whether other bromodomain proteins are sufficient to increase transcript levels at the *EP1* locus. The system can also be used to help characterize the many chromatin associated proteins found in complexes that localize to transcription start sites (26).

Materials and Methods

Strain details and culture growth

Bloodstream SM *EP1/GFP* parasites (51) were cultured in HMI-9 (88) at 37°C and 5% CO_2. The dCas9-Bdf3 fusion construct, the dCas9 alone construct, and the Bdf3 alone

471 constructs were transfected into reporter parasites using an AMAXA nucleofector with the
472 X-001 setting. For each transfection, 30-50 million parasites were harvested and
473 resuspended in 100 uL of nucleofector T cell solution with 5-10 μg of NotI-linearized
474 plasmid (New England Biolabs). Parasites were grown for 6 days in culture medium and
475 selected for resistance using 5.0μg/ml Blasticidin. T7 promoter driven guide RNA
476 constructs were linearized and introduced using the same method except 2.5μg/ml
477 phleomycin was used for selection. Expression of each introduced protein was confirmed
478 by western blot (see below).
479
480 **Plasmid construction**
481
482 The plasmid containing the dCas9 Bdf3 fusion sequence was constructed in two halves:
483 the first half consisted of the 3X FLAG tag, La Nuclear Localization Signal (89), and the
484 front half of the dCas9 coding region, and the second half consisted of the back half of
485 the dCas9 coding region, the GS linker, and the Bdf3 coding region. Both halves were
486 synthesized by Twist Biosciences. The front 3X Flag/La NLS/dCas9 coding region was
487 amplified using Forward ggccaagcttatggactacaaggaccac and Reverse
488 gcgcgggcccacgtagtacggg primers containing HindIII (New England Biolabs) and ApaI
489 (New England Biolabs) restriction enzyme recognition sites. This section was digested
490 with HindIII and ApaI and cloned into a pLEW100 vector at these same sites. The back
491 dCas9/Glycine-Serine linker/Bdf3 coding region was cut with ApaI and BamHI (New
492 England Biolabs) and cloned into the pLEW100/3X Flag/La NLS/dCas9 vector at the ApaI
493 and BamHI sites within the vector.
494
495 **sgRNA construction**
496
497 Complementary single-stranded oligos were engineered with BbsI overhangs. Oligos
498 were combined at a concentration of 5μM each in TE buffer with a reaction volume of
499 50μL. The oligos were annealed in a thermocycler as follows: 93°C for 0:01 with a ramp
500 time of 3 °C/s, 70 °C for 3:00 with a ramp time of 3 °C/s, and a hold at 4°C with a ramp
501 time of 0.1 °C/s. pT7sgRNA (56) was a gift from David Horn (Addgene plasmid # 111820
502 ; http://n2t.net/addgene:111820 ; RRID:Addgene_111820). pT7sgRNA vector was
503 linearized with BbsI-HF (New England Biolabs) and purified. 150 ng of linearized
504 pT7sgRNA and annealed oligo at a concentration of 2 μM of were ligated together using
505 quick ligase (New England Biolabs) in a 20μL reaction for 5 minutes at 25ºC. Ligated
506 plasmids were transformed into electrocompetent cells to screen for correct integration of
507 the oligos. The oligo sequences used were: EP1-1 forward, agggtgggcgtgcattgaaaatag;
508 EP1-1 reverse, aaacctattttcaatgcacgccca; EP1-3 forward, aggggctgttccgtgtctctgggt; EP1-
509 3 reverse, aaacacccagagacacggaacagc; Neo1 forward, aggggatctggacgaagagcatca;
510 Neo1 reverse, aaactgatgctcttcgtccagatc.
511
512
513
514

515
516 **Western Blotting**
517
518 SM *EPI/GFP* dCas9-Bdf3, dCas9 alone, or Bdf3 alone parasites were treated with or
519 without 1 μg/mL dox and 8 million parasites were harvested after 48h or 72h of treatment.
520 Harvested parasites were resuspended in 2X Laemmli buffer and boiled at 95°C for 10
521 minutes. The samples were loaded onto a 4-20% gradient polyacrylamide gel and protein
522 was transferred to the PVDF membrane. The membrane was blocked in 7 mL of 5% milk
523 in Tris-Buffered Saline (TBS), then incubated overnight at 4°C in M2 mouse anti-FLAG
524 (Sigma), rabbit anti-FLAG (Cell Signaling), or the control anti-tubulin (a kind gift from
525 George Cross) in 5% milk in (TBS) at a 1:1000 dilution. After 3 washes in TBS with 0.1%
526 Tween-20, the membrane was incubated at room temperature for 1 hr in goat anti-mouse
527 or goat anti-rabbit fluorescently labeled antibody (Biorad) at a 1:10000 dilution in 5% milk
528 in TBS. After all antibody incubations, the membrane was washed three times in TBS
529 with 0.1% Tween-20 and a final wash in TBS alone. The membrane was imaged on a LI-
530 COR Odyssey instrument.
531
532 **Flow cytometry**
533
534 SM *EPI/GFP* dCas9-Bdf3 or dCas9 cells were prepared at a density of 15,000 cell/mL
535 and treated with or without 1 µg/mL dox in 2 mL of culture medium. Parasites were diluted
536 in fresh media with dox as needed to maintain them under 1 million/ml. After two and
537 three days of growth, 1 mL of culture was harvested and analyzed by flow cytometry for
538 *EP1/GFP* expression. All samples were analyzed with a Novocyte 2000R from Acea
539 Biosciences.
540
541 **Analysis of parasite growth**
542
543 Parasites were prepared at a density of 100,000 cells/mL and grown in 96 well plates with
544 a starting volume of 200μL HMI-9 medium for 24h with or without 1 μg/mL dox. After 24
545 hours of growth, 20 μL of culture was analyzed by flow cytometry and the number of
546 parasites in the live gate was calculated. Cultures were diluted back down to 100,000
547 cell/mL using the number of cells determined by the live gate. This procedure occured
548 daily for a total of 5 days.
549
550 **Quantitative PCR**
551
552 RNA was isolated from parasites using the Direct-zol RNA MiniPrep kit from Genesee,
553 which includes DNAse treatment. cDNA was generated using the SuperScript IV VILO
554 Master Mix (Fisher Scientific) according to the manufacturer's instructions starting with
555 1μg of RNA. cDNA was amplified with primers combined with 2X Sybr green master
556 mix (Life Technologies) and analyzed on an Eppendorf Realplex2 instrument. Primers
557 used were as follows: Tb427.10.10260 EP1, tctgctcgctattcttctgttc,
558 cctttgcctcccttagtaagac, Tb927.6.510 GPEET agtcggctagcaacgttatc, ttctggtccggtctcttct,

559 Tb927.9.11600, GIM5B, ttgcgaggatgggtgatg, gggtttggagagggaagttaat, Tb927.10.2010,
560 HK1, gtcagcacttactcccatcaa, acgacgcatcgtcaatatcc, Tb927.10.5620, ALD,
561 gtctgaagctgttgttcgtttc, cacctcaggctccacaatag, Tb927.10.10220, PAG2,
562 aggagatacgaggaatgagaca, tcttcaaacgcccggtaag, Tb927.10.14140 PYK1,
563 gagaaggttggcacaaagga, tcacaccgtcgtcaacataaa, GFP, ctacaacagccacaaggtctat,
564 ggtgttctgctggtagtg, Tb927.10.9400, SF1, ggtatggttcatcaggagttgg,
565 cgttagcactggtatccttcag.
566
567
568 **Accession numbers**
569 EP1, Tb927.10.10260
570 PAG2, Tb927.10.10220
571 GPEET, Tb927.6.510
572 HK1, Tb927.10.2010
573 GIM5B, Tb927.9.11600
574 ALD, Tb927.10.5620
575 PYK1, Tb927.10.14140
576 SF1, Tb927.10.9400
577 BDF3, Tb927.11.10070
578
579
580 ## Acknowledgements.
581
582 We would like to acknowledge Monica Mugnier, who provided excellent advice on
583 adapting existing CRISPR-Cas9 systems to *T. brucei*. D.S. is supported by a NSF
584 CAREER grant (2041395), which also supported the undergraduate students who worked
585 on the project.
586
587
588 **References**
589
590 1. Alsan M. 2015. The Effect of the TseTse Fly on African Development. American
591 Economic Review 105:382–410.

592 2. Shaw APM, Cecchi G, Wint GRW, Mattioli RC, Robinson TP. 2014. Mapping the
593 economic benefits to livestock keepers from intervening against bovine
594 trypanosomosis in Eastern Africa. Preventive Veterinary Medicine 113:197–210.

595 3. Cross GAM, Kim H-S, Wickstead B. 2014. Capturing the variant surface
596 glycoprotein repertoire (the VSGnome) of Trypanosoma brucei Lister 427.
597 Molecular & Biochemical Parasitology 195:59–73.

598 4. Van Hellemond JJ, Bakker BM, Tielens AGM. 2005. Energy Metabolism and Its
599 Compartmentation in Trypanosoma brucei, p. 199–226. *In* Advances in Microbial
600 Physiology. Elsevier.

601 5. Van Grinsven KWA, Van Den Abbeele J, Van Den Bossche P, Van Hellemond JJ,
602 Tielens AGM. 2009. Adaptations in the Glucose Metabolism of Procyclic
603 *Trypanosoma brucei* Isolates from Tsetse Flies and during Differentiation of
604 Bloodstream Forms. Eukaryot Cell 8:1307–1311.

605 6. Flynn IW, Bowman IBR. 1973. The metabolism of carbohydrate by pleomorphic
606 African trypanosomes. Comparative Biochemistry and Physiology Part B:
607 Comparative Biochemistry 45:25–42.

608 7. Hannaert V, Bringaud F, Opperdoes FR, Michels PA. 2003. Evolution of energy
609 metabolism and its compartmentation in Kinetoplastida. Kinetoplastid Biol Dis 2:11.

610 8. Roditi I, Carrington M, Turner M. 1987. Expression of a polypeptide containing a
611 dipeptide repeat is confined to the insect stage of Trypanosoma brucei. Nature
612 325:272–274.

613 9. Roditi I, Schwarz H, Pearson TW, Beecroft RP, Liu MK, Richardson JP, Bühring
614 HJ, Pleiss J, Bülow R, Williams RO. 1989. Procyclin gene expression and loss of

615 the variant surface glycoprotein during differentiation of Trypanosoma brucei. The
616 Journal of cell biology 108:737–746.

617 10. Vassella E, Acosta-Serrano A, Studer E, Lee SH, Englund PT, Roditi I. 2001.
618 Multiple procyclin isoforms are expressed differentially during the development of
619 insect forms of Trypanosoma brucei. J Mol Biol 312:597–607.

620 11. Acosta-Serrano A, Vassella E, Liniger M, Renggli CK, Brun R, Roditi I, Englund PT.
621 2001. The surface coat of procyclic *Trypanosoma brucei:* Programmed expression
622 and proteolytic cleavage of procyclin in the tsetse fly. Proc Natl Acad Sci USA
623 98:1513–1518.

624 12. Clayton CE, Fueri JP, Itzhaki JE, Bellofatto V, Sherman DR, Wisdom GS,
625 Vijayasarathy S, Mowatt MR. 1990. Transcription of the procyclic acidic repetitive
626 protein genes of Trypanosoma brucei. Mol Cell Biol 10:3036–3047.

627 13. Biebinger S, Rettenmaier S, Flaspohler J, Hartmann C, Peña-Diaz J, Wirtz LE,
628 Hotz HR, Barry JD, Clayton C. 1996. The PARP promoter of Trypanosoma brucei
629 is developmentally regulated in a chromosomal context. Nucleic Acids Res
630 24:1202–1211.

631 14. Brown SD, Huang J, Van der Ploeg LH. 1992. The promoter for the procyclic acidic
632 repetitive protein (PARP) genes of Trypanosoma brucei shares features with RNA
633 polymerase I promoters. Mol Cell Biol 12:2644–2652.

634 15. Gunzl A, Bruderer T, Laufer G, Schimanski B, Tu LC, Chung HM, Lee PT, Lee
635 MGS. 2003. RNA Polymerase I Transcribes Procyclin Genes and Variant Surface
636 Glycoprotein Gene Expression Sites in Trypanosoma brucei. Eukaryotic Cell
637 2:542–551.

638 16. Rudenko G, Lee MG, Van der Ploeg LH. 1992. The PARP and VSG genes of
639 Trypanosoma brucei do not resemble RNA polymerase II transcription units in
640 sensitivity to Sarkosyl in nuclear run-on assays. Nucleic Acids Res 20:303–306.

641 17. Clayton CE. 2016. Gene expression in Kinetoplastids. Current Opinion in
642 Microbiology 32:46–51.

643 18. Luzak V, Osses E, Danese A, Odendaal C, Cosentino RO, Stricker SH, Haanstra
644 JR, Erhard F, Siegel TN. 2025. SLAM-seq reveals independent contributions of
645 RNA processing and stability to gene expression in African trypanosomes. Nucleic
646 Acids Research 53:gkae1203.

647 19. Jenuwein T, Allis CD. 2001. Translating the Histone Code. Science 293:1074–
648 1080.

649 20. Maree JP, Tvardovskiy A, Ravnsborg T, Jensen ON, Rudenko G, Patterton H-G.
650 2022. *Trypanosoma brucei* histones are heavily modified with combinatorial post-
651 translational modifications and mark Pol II transcription start regions with
652 hyperacetylated H2A. Nucleic Acids Research 50:9705–9723.

653 21. Siegel TN, Hekstra DR, Kemp LE, Figueiredo LM, Lowell JE, Fenyo D, Wang X,
654 Dewell S, Cross GAM. 2009. Four histone variants mark the boundaries of
655 polycistronic transcription units in Trypanosoma brucei. Genes & Development
656 23:1063–1076.

657 22. Kawahara T, Siegel TN, Ingram AK, Alsford S, Cross GAM, Horn D. 2008. Two
658 essential MYST-family proteins display distinct roles in histone H4K10 acetylation
659 and telomeric silencing in trypanosomes. Molecular Microbiology 69:1054–1068.

660 23. Siegel TN, Kawahara T, DeGrasse JA, Janzen CJ, Horn D, Cross GAM. 2007.
661 Acetylation of histone H4K4 is cell cycle regulated and mediated by HAT3 in
662 Trypanosoma brucei. Molecular Microbiology 67:762–771.

663 24. Wang Q-P, Kawahara T, Horn D. 2010. Histone deacetylases play distinct roles in
664 telomeric VSG expression site silencing in African trypanosomes. Molecular
665 Microbiology 77:1237–1245.

666 25. Schulz D, Mugnier MR, Paulsen E-M, Kim H-S, Chung CW, Tough DF, Rioja I,
667 Prinjha RK, Papavasiliou FN, Debler EW. 2015. Bromodomain Proteins Contribute
668 to Maintenance of Bloodstream Form Stage Identity in the African Trypanosome.
669 PLoS Biol 13:e1002316-38.

670 26. Staneva DP, Carloni R, Auchynnikava T, Tong P, Rappsilber J, Jeyaprakash AA,
671 Matthews KR, Allshire RC. 2021. A systematic analysis of *Trypanosoma brucei*

672 chromatin factors identifies novel protein interaction networks associated with sites
673 of transcription initiation and termination. Genome Res 31:2138–2154.

674 27. Frederiks F, van Welsem T, Oudgenoeg G, Heck AJR, Janzen CJ, van Leeuwen F.
675 2010. Heterologous expression reveals distinct enzymatic activities of two DOT1
676 histone methyltransferases of Trypanosoma brucei. Journal of Cell Science
677 123:4019–4023.

678 28. Figueiredo LM, Janzen CJ, Cross GAM. 2008. A histone methyltransferase
679 modulates antigenic variation in African trypanosomes. PLoS Biol 6:e161.

680 29. Tamkun JW, Deuring R, Scott MP, Kissinger M, Pattatucci AM, Kaufman TC,
681 Kennison JA. 1992. brahma: A regulator of Drosophila homeotic genes structurally
682 related to the yeast transcriptional activator SNF2SWI2. Cell 68:561–572.

683 30. Haynes SR, Dollard C, Winston F, Beck S, Trowsdale J, Dawid IB. 1992. The
684 bromodomain: a conserved sequence found in human, *Drosophila* and yeast
685 proteins. Nucl Acids Res 20:2603–2603.

686 31. Brownell JE, Zhou J, Ranalli T, Kobayashi R, Edmondson DG, Roth SY, Allis CD.
687 1996. Tetrahymena Histone Acetyltransferase A: A Homolog to Yeast Gcn5p
688 Linking Histone Acetylation to Gene Activation. Cell 84:843–851.

689 32. Ogryzko VV, Schiltz RL, Russanova V, Howard BH, Nakatani Y. 1996. The
690 Transcriptional Coactivators p300 and CBP Are Histone Acetyltransferases. Cell
691 87:953–959.

692 33. Bannister AJ, Kouzarides T. 1996. The CBP co-activator is a histone
693 acetyltransferase. Nature 384:641–643.

694 34. Di Micco R, Fontanals-Cirera B, Low V, Ntziachristos P, Yuen SK, Lovell CD,
695 Dolgalev I, Yonekubo Y, Zhang G, Rusinova E, Gerona-Navarro G, Cañamero M,
696 Ohlmeyer M, Aifantis I, Zhou M-M, Tsirigos A, Hernando E. 2014. Control of
697 Embryonic Stem Cell Identity by BRD4-Dependent Transcriptional Elongation of
698 Super-Enhancer-Associated Pluripotency Genes. Cell Reports 9:234–247.

699 35. Rodriguez RM, Suarez-Alvarez B, Salvanés R, Huidobro C, Toraño EG, Garcia-
700 Perez JL, Lopez-Larrea C, Fernandez AF, Bueno C, Menendez P, Fraga MF.
701 2014. Role of BRD4 in hematopoietic differentiation of embryonic stem cells.
702 Epigenetics 9:566–578.

703 36. Horne GA, Stewart HJS, Dickson J, Knapp S, Ramsahoye B, Chevassut T. 2015.
704 Nanog requires BRD4 to maintain murine embryonic stem cell pluripotency and is
705 suppressed by bromodomain inhibitor JQ1 together with Lefty1. Stem Cells Dev
706 24:879–891.

707 37. Fleck K, McNutt S, Chu F, Jeffers V. 2023. An apicomplexan bromodomain protein,
708 TgBDP1, associates with diverse epigenetic factors to regulate essential
709 transcriptional processes in *Toxoplasma gondii*. mBio e03573-22.

710 38. Jones NG, Geoghegan V, Moore G, Carnielli JBT, Newling K, Calderón F, Gabarró
711 R, Martín J, Prinjha RK, Rioja I, Wilkinson AJ, Mottram JC. 2022. Bromodomain

712 factor 5 is an essential regulator of transcription in Leishmania. Nat Commun
713 13:4071.

714 39. Alonso VL, Villanova GV, Ritagliati C, Machado Motta MC, Cribb P, Serra EC.
715 2014. Trypanosoma cruzi Bromodomain Factor 3 Binds Acetylated α-Tubulin and
716 Concentrates in the Flagellum during Metacyclogenesis. Eukaryot Cell 13:822–
717 831.

718 40. Alonso VL, Ritagliati C, Cribb P, Cricco J, Serra E. 2016. Overexpression of
719 bromodomain factor 3 in Trypanosoma cruzi(TcBDF3) affects parasite
720 differentiation and protects it against bromodomain inhibitors. FEBS J n/a-n/a.

721 41. Tang J, Yeoh LM, Grotz MD, Goodman CD, Chisholm SA, Nguyen HHT, Yu C,
722 Pareek K, McPherson F, Cozijnsen A, Hustadt SA, Josling GA, Day KP, Schulz D,
723 McFadden GI, de Koning-Ward TF, Petter M, Duffy MF. 2025. *Pf*GCN5 is essential
724 for *Plasmodium falciparum* survival and transmission and regulates Pf H2B.Z
725 acetylation and chromatin structure. Nucleic Acids Research 53.

726 42. Miao J, Wang C, Lucky AB, Liang X, Min H, Adapa SR, Jiang R, Kim K, Cui L.
727 2021. A unique GCN5 histone acetyltransferase complex controls erythrocyte
728 invasion and virulence in the malaria parasite Plasmodium falciparum. PLoS
729 Pathog 17:e1009351.

730 43. Tian J, Dai B, Gong L, Wang P, Ding H, Xia S, Sun W, Ren C, Shen J, Liu M. 2022.
731 JQ-1 ameliorates schistosomiasis liver granuloma in mice by suppressing male and

732 female reproductive systems and egg development of Schistosoma japonicum.
733 PLoS Negl Trop Dis 16:e0010661.

734 44. Ashby EC, Havens JL, Rollosson LM, Hardin J, Schulz D. 2023. Chemical
735 Inhibition of Bromodomain Proteins in Insect-Stage African Trypanosomes Perturbs
736 Silencing of the Variant Surface Glycoprotein Repertoire and Results in
737 Widespread Changes in the Transcriptome. Microbiol Spectr 11:e0014723.

738 45. Figueiredo LM, Cross GAM, Janzen CJ. 2009. Epigenetic regulation in African
739 trypanosomes: a new kid on the block. Nature Publishing Group 7:504–513.

740 46. Miller G, Rollosson LM, Saada C, Wade SJ, Schulz D. 2023. Adaptation of
741 CUT&RUN for use in African trypanosomes. PLoS One 18:e0292784.

742 47. Ziegelbauer K, Quinten M, Schwarz H, Pearson TW, Overath P. 1990.
743 Synchronous differentiation of Trypanosoma brucei from bloodstream to procyclic
744 forms in vitro. Eur J Biochem 192:373–378.

745 48. Ashby E, Paddock L, Betts HL, Liao J, Miller G, Porter A, Rollosson LM, Saada C,
746 Tang E, Wade SJ, Hardin J, Schulz D. 2022. Genomic Occupancy of the
747 Bromodomain Protein Bdf3 Is Dynamic during Differentiation of African
748 Trypanosomes from Bloodstream to Procyclic Forms. mSphere 7:e0002322.

749 49. Gilbert LA, Larson MH, Morsut L, Liu Z, Brar GA, Torres SE, Stern-Ginossar N,
750 Brandman O, Whitehead EH, Doudna JA, Lim WA, Weissman JS, Qi LS. 2013.

751 CRISPR-Mediated Modular RNA-Guided Regulation of Transcription in
752 Eukaryotes. Cell 154:442–451.

753 50. Gilbert LA, Horlbeck MA, Adamson B, Villalta JE, Chen Y, Whitehead EH,
754 Guimaraes C, Panning B, Ploegh HL, Bassik MC, Qi LS, Kampmann M, Weissman
755 JS. 2014. Genome-Scale CRISPR-Mediated Control of Gene Repression and
756 Activation. Cell 159:647–661.

757 51. Walsh ME, Naudzius EM, Diaz SJ, Wismar TW, Martchenko Shilman M, Schulz D.
758 2020. Identification of clinically approved small molecules that inhibit growth and
759 affect transcript levels of developmentally regulated genes in the African
760 trypanosome. PLoS Negl Trop Dis 14:e0007790.

761 52. Chen X, Zaro JL, Shen W-C. 2013. Fusion protein linkers: Property, design and
762 functionality. Advanced Drug Delivery Reviews 65:1357–1369.

763 53. Qi LS, Larson MH, Gilbert LA, Doudna JA, Weissman JS, Arkin AP, Lim WA. 2013.
764 Repurposing CRISPR as an RNA-Guided Platform for Sequence-Specific Control
765 of Gene Expression. Cell 152:1173–1183.

766 54. Pfeiffer ML, Winkler J, Van Damme D, Jacobs TB, Nowack MK. 2022. Conditional
767 and tissue-specific approaches to dissect essential mechanisms in plant
768 development. Current Opinion in Plant Biology 65:102119.

769 55. Xiao B, Yin S, Hu Y, Sun M, Wei J, Huang Z, Wen Y, Dai X, Chen H, Mu J, Cui L,
770 Jiang L. 2019. Epigenetic editing by CRISPR/dCas9 in *Plasmodium falciparum*.
771 Proc Natl Acad Sci USA 116:255–260.

772 56. Rico E, Jeacock L, Kovářová J, Horn D. 2018. Inducible high-efficiency CRISPR-
773 Cas9-targeted gene editing and precision base editing in African trypanosomes.
774 Sci Rep 8:1–10.

775 57. Shaw S, Knüsel S, Hoenner S, Roditi I. 2020. A transient CRISPR/Cas9 expression
776 system for genome editing in Trypanosoma brucei. BMC Res Notes 13:268.

777 58. Beneke T, Madden R, Makin L, Valli J, Sunter J, Gluenz E. 2017. A CRISPR Cas9
778 high-throughput genome editing toolkit for kinetoplastids. R Soc open sci 4:170095.

779 59. Wirtz E, Leal S, Ochatt C, Cross GA. 1999. A tightly regulated inducible expression
780 system for conditional gene knock-outs and dominant-negative genetics in
781 Trypanosoma brucei. Mol Biochem Parasitol 99:89–101.

782 60. Huang J, Van Der Ploeg LH. 1991. Requirement of a polypyrimidine tract for trans-
783 splicing in trypanosomes: discriminating the PARP promoter from the immediately
784 adjacent 3′ splice acceptor site. The EMBO Journal 10:3877–3885.

785 61. Peng D, Tarleton R. 2015. EuPaGDT: a web tool tailored to design CRISPR guide
786 RNAs for eukaryotic pathogens. Microbial Genomics 1.

787 62. Pena AC, Pimentel MR, Manso H, Vaz-Drago R, Pinto-Neves D, Aresta-Branco F,
788 Rijo-Ferreira F, Guegan F, Pedro Coelho L, Carmo-Fonseca M, Barbosa-Morais

789 NL, Figueiredo LM. 2014. *T rypanosoma brucei* histone H 1 inhibits RNA
790 polymerase I transcription and is important for parasite fitness *in vivo*. Molecular
791 Microbiology 93:645–663.

792 63. Glover L, Hutchinson S, Alsford S, Horn D. 2016. VEX1 controls the allelic
793 exclusion required for antigenic variation in trypanosomes. Proceedings of the
794 National Academy of Sciences 1–6.

795 64. Aresta-Branco F, Sanches-Vaz M, Bento F, Rodrigues JA, Figueiredo LM. 2019.
796 African trypanosomes expressing multiple VSGs are rapidly eliminated by the host
797 immune system. Proc Natl Acad Sci USA 116:20725–20735.

798 65. Batram C, Jones NG, Janzen CJ, Markert SM, Engstler M. 2014. Expression site
799 attenuation mechanistically links antigenic variation and development in
800 Trypanosoma brucei. eLife 3:e02324.

801 66. Rico E, Rojas F, Mony BM, Szőőr B, MacGregor P, Matthews KR. 2013.
802 Bloodstream form pre-adaptation to the tsetse fly in Trypanosoma brucei. Front
803 Cell Infect Microbiol 3:78.

804 67. Wenzler T, Schumann Burkard G, Schmidt RS, Mäser P, Bergner A, Roditi I, Brun
805 R. 2016. A new approach to chemotherapy: drug-induced differentiation kills
806 African trypanosomes. Sci Rep 6:22451.

807 68. Kabani S, Fenn K, Ross A, Ivens A, Smith TK, Ghazal P, Matthews K. 2009.
808 Genome-wide expression profiling of in vivo-derived bloodstream parasite stages

809 and dynamic analysis of mRNA alterations during synchronous differentiation in
810 Trypanosoma brucei. BMC Genomics 10:427.

811 69. Queiroz R, Benz C, Fellenberg K, Hoheisel JD, Clayton C. 2009. Transcriptome
812 analysis of differentiating trypanosomes reveals the existence of multiple post-
813 transcriptional regulons. BMC Genomics 10:495.

814 70. Furger A, Schürch N, Kurath U, Roditi I. 1997. Elements in the 3' untranslated
815 region of procyclin mRNA regulate expression in insect forms of Trypanosoma
816 brucei by modulating RNA stability and translation. Molecular and Cellular Biology
817 17:4372–4380.

818 71. Hehl A, Vassella E, Braun R, Roditi I. 1994. A conserved stem-loop structure in the
819 3' untranslated region of procyclin mRNAs regulates expression in Trypanosoma
820 brucei. Proc Natl Acad Sci USA 91:370–374.

821 72. Vassella E, Den Abbeele JV, Bütikofer P, Renggli CK, Furger A, Brun R, Roditi I.
822 2000. A major surface glycoprotein of *Trypanosoma brucei* is expressed transiently
823 during development and can be regulated post-transcriptionally by glycerol or
824 hypoxia. Genes Dev 14:615–626.

825 73. Walrad P, Paterou A, Acosta-Serrano A, Matthews KR. 2009. Differential
826 Trypanosome Surface Coat Regulation by a CCCH Protein That Co-Associates
827 with procyclin mRNA cis-Elements. PLoS Pathog 5:e1000317.

828 74. Walrad PB, Capewell P, Fenn K, Matthews KR. 2012. The post-transcriptional
829 trans-acting regulator, TbZFP3, co-ordinates transmission-stage enriched mRNAs
830 in Trypanosoma brucei. Nucleic Acids Res 40:2869–2883.

831 75. Morris JC, Wang Z, Drew ME, Englund PT. 2002. Glycolysis modulates
832 trypanosome glycoprotein expression as revealed by an RNAi library. EMBO J
833 21:4429–4438.

834 76. Filippakopoulos P, Picaud S, Mangos M, Keates T, Lambert J-P, Barsyte-Lovejoy
835 D, Felletar I, Volkmer R, Müller S, Pawson T, Gingras A-C, Arrowsmith CH, Knapp
836 S. 2012. Histone Recognition and Large-Scale Structural Analysis of the Human
837 Bromodomain Family. Cell 149:214–231.

838 77. Kraus AJ, Vanselow JT, Lamer S, Brink BG, Schlosser A, Siegel TN. 2020. Distinct
839 roles for H4 and H2A.Z acetylation in RNA transcription in African trypanosomes.
840 Nat Commun 11:1498.

841 78. Vellmer T, Hartleb L, Fradera Sola A, Kramer S, Meyer-Natus E, Butter F, Janzen
842 CJ. 2022. A novel SNF2 ATPase complex in Trypanosoma brucei with a role in
843 H2A.Z-mediated chromatin remodelling. PLoS Pathog 18:e1010514.

844 79. Trenaman A, Tinti M, Wall RJ, Horn D. 2024. Post-transcriptional reprogramming
845 by thousands of mRNA untranslated regions in trypanosomes. Nat Commun
846 15:8113.

847 80. Wilson K, Uyetake L, Boothroyd J. 1999. Trypanosoma brucei: Cis-Acting
848 Sequences Involved in the Developmental Regulation of PARP Expression.
849 Experimental Parasitology 91:222–230.

850 81. Rajan KS, Adler K, Madmoni H, Peleg-Chen D, Cohen-Chalamish S, Doniger T,
851 Galili B, Gerber D, Unger R, Tschudi C, Michaeli S. 2021. Pseudouridines on
852 *Trypanosoma brucei* mRNAs are developmentally regulated: Implications to mRNA
853 stability and protein binding. Molecular Microbiology 116:808–826.

854 82. Galili-Kostin B, Rajan KS, Ida Ashkenazi Y, Freedman A, Doniger T, Cohen-
855 Chalamish S, Waldman Ben-Asher H, Unger R, Roditi I, Tschudi C, Michaeli S.
856 2025. TblncRNA-23, a long non-coding RNA transcribed by RNA polymerase I,
857 regulates developmental changes in Trypanosoma brucei. Nat Commun 16:3697.

858 83. Bard JE, Tylec BL, Dubey AP, Lamb NA, Yergeau DA, Read LK. 2024. Life stage–
859 specific poly(A) site selection regulated by *Trypanosoma brucei* DRBD18. Proc
860 Natl Acad Sci USA 121:e2403188121.

861 84. Radzisheuskaya A, Shlyueva D, Müller I, Helin K. 2016. Optimizing sgRNA position
862 markedly improves the efficiency of CRISPR/dCas9-mediated transcriptional
863 repression. Nucleic Acids Res 44:e141–e141.

864 85. Sundaresan R, Parameshwaran HP, Yogesha SD, Keilbarth MW, Rajan R. 2017.
865 RNA-Independent DNA Cleavage Activities of Cas9 and Cas12a. Cell Reports
866 21:3728–3739.

867 86. Dhalluin C, Carlson JE, Zeng L, He C, Aggarwal AK, Zhou M-M, Zhou M-M. 1999.
868 Structure and ligand of a histone acetyltransferase bromodomain. Nature 399:491–
869 496.

870 87. Mujtaba S, Zeng L, Zhou M-M. 2007. Structure and acetyl-lysine recognition of the
871 bromodomain. Oncogene 26:5521–5527.

872 88. Hirumi H, Hirumi K. 1989. Continuous cultivation of Trypanosoma brucei blood
873 stream forms in a medium containing a low concentration of serum protein without
874 feeder cell layers. J Parasitol 75:985–989.

875 89. Gunaratne L, Moore H, Albaum N, Casius A, Henderson J, Kessler A, Hegedűsová
876 E, Kulkarni S, Arthur H, Ross RL, Paris Z, Maraia R, Lowe TM, Alfonzo JD. 2025.
877 Key RNA-binding domains in the La protein establish tRNA modification levels in
878 Trypanosoma brucei. Nucleic Acids Res 53:gkaf594.

879
880
881

A.

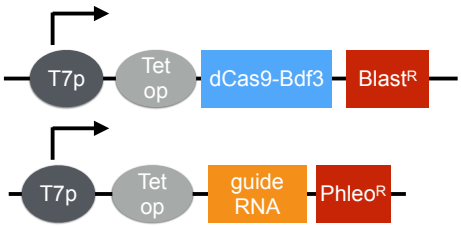
T7p
Tet op
dCas9-Bdf3
Blast^R
T7p
Tet op
guide RNA
Phleo^R

B.

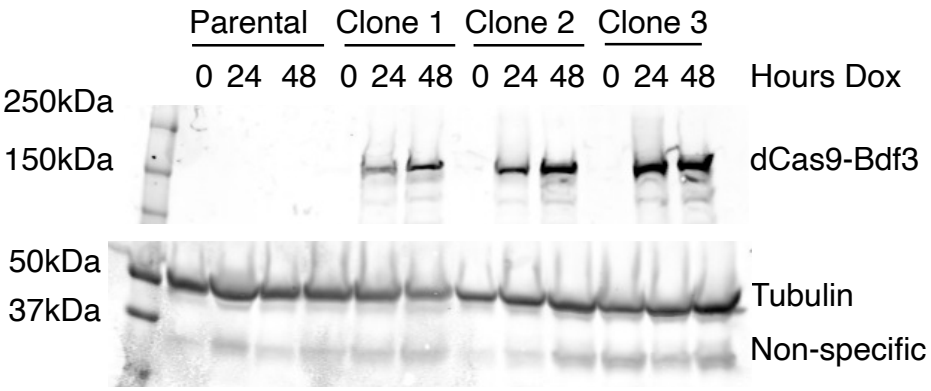
Parental
Clone 1
Clone 2
Clone 3
0 24 48 0 24 48 0 24 48 0 24 48
Hours Dox
250kDa
150kDa
dCas9-Bdf3
50kDa
37kDa
Tubulin
Non-specific

C.

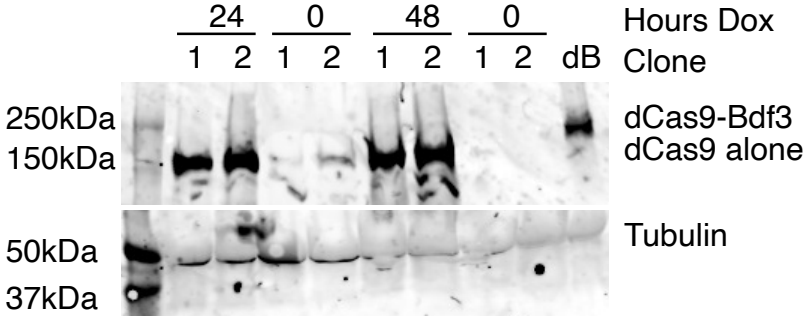
24
0
48
0
Hours Dox
1 2 1 2 1 2 1 2 dB
Clone
250kDa
150kDa
dCas9-Bdf3
dCas9 alone
50kDa
37kDa
Tubulin

D.

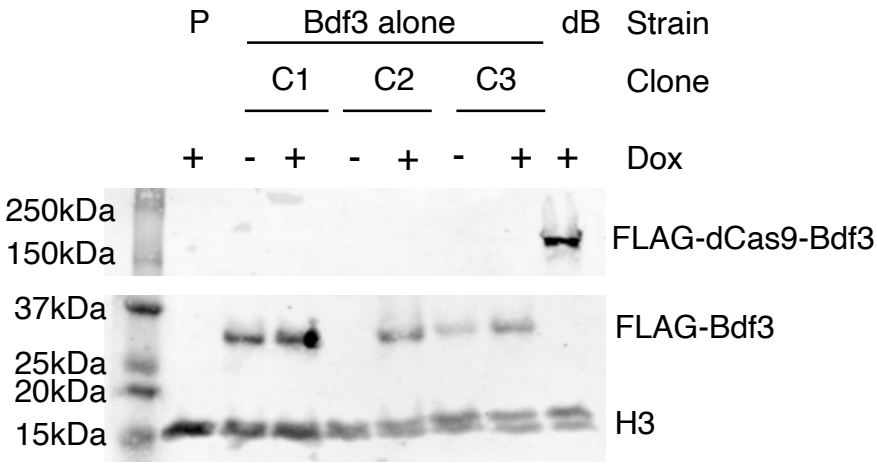
P
Bdf3 alone
dB
Strain
C1
C2
C3
Clone
+ - + - + - + +
Dox
250kDa
150kDa
FLAG-dCas9-Bdf3
37kDa
25kDa
20kDa
15kDa
FLAG-Bdf3
H3

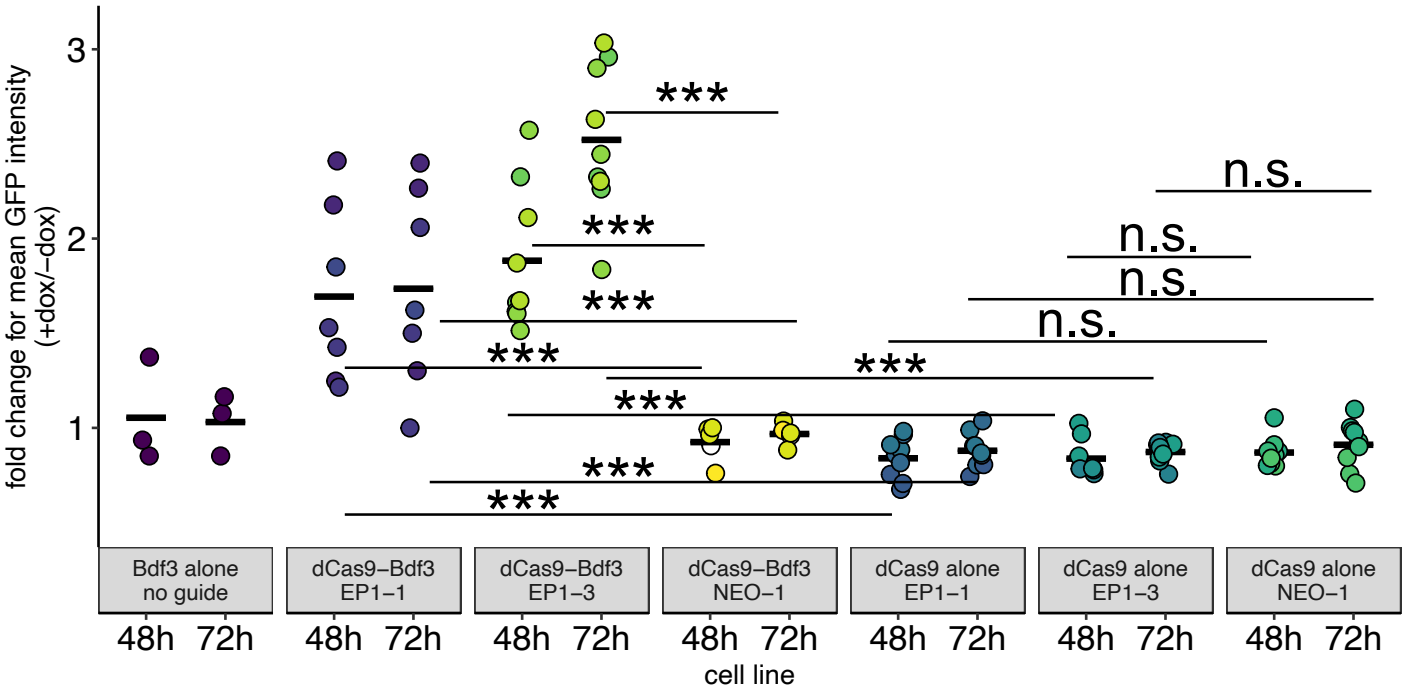
fold change for mean GFP intensity
(+dox/−dox)
3
2
1
***
***
***
***
***
***
***
***
n.s.
n.s.
n.s.
n.s.
Bdf3 alone
no guide
dCas9−Bdf3
EP1−1
dCas9−Bdf3
EP1−3
dCas9−Bdf3
NEO−1
dCas9 alone
EP1−1
dCas9 alone
EP1−3
dCas9 alone
NEO−1
48h 72h
cell line

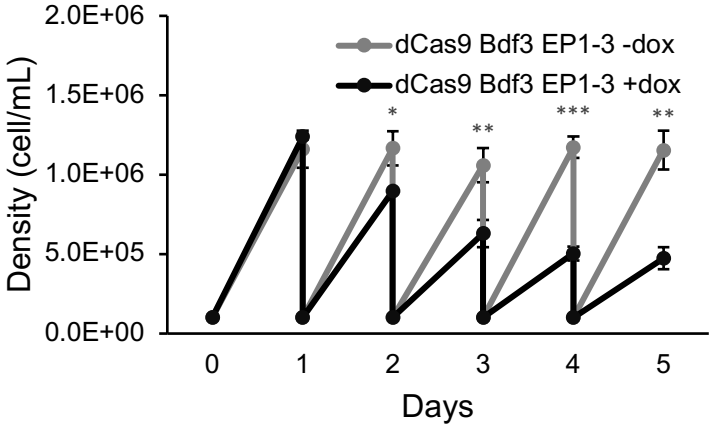
dCas9 Bdf3 EP1-3 -dox
dCas9 Bdf3 EP1-3 +dox
Density (cell/mL)
2.0E+06
1.5E+06
1.0E+06
5.0E+05
0.0E+00
*
**
***
**
0
1
2
3
4
5
Days

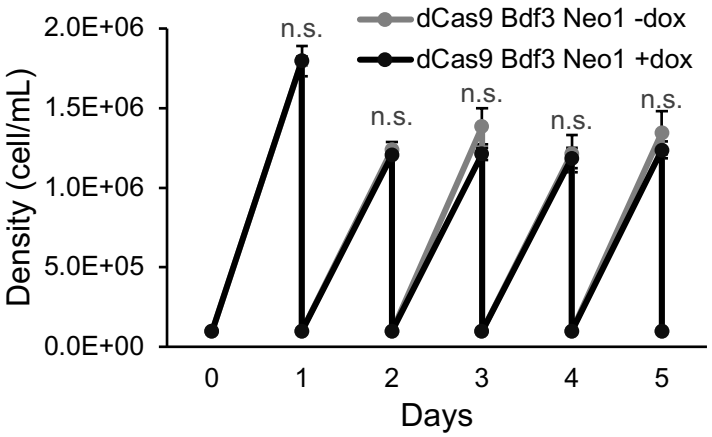
dCas9 Bdf3 Neo1 -dox
dCas9 Bdf3 Neo1 +dox
Density (cell/mL)
2.0E+06
1.5E+06
1.0E+06
5.0E+05
0.0E+00
n.s.
n.s.
n.s.
n.s.
n.s.
0
1
2
3
4
5
Days

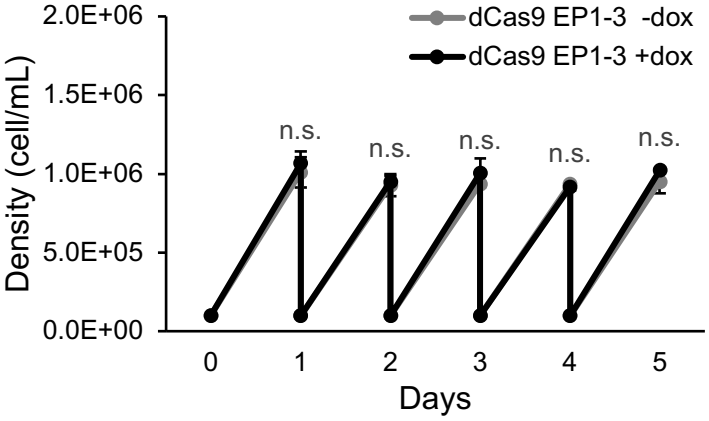
dCas9 EP1-3 -dox
dCas9 EP1-3 +dox
Density (cell/mL)
2.0E+06
1.5E+06
1.0E+06
5.0E+05
0.0E+00
n.s.
n.s.
n.s.
n.s.
n.s.
0
1
2
3
4
5
Days

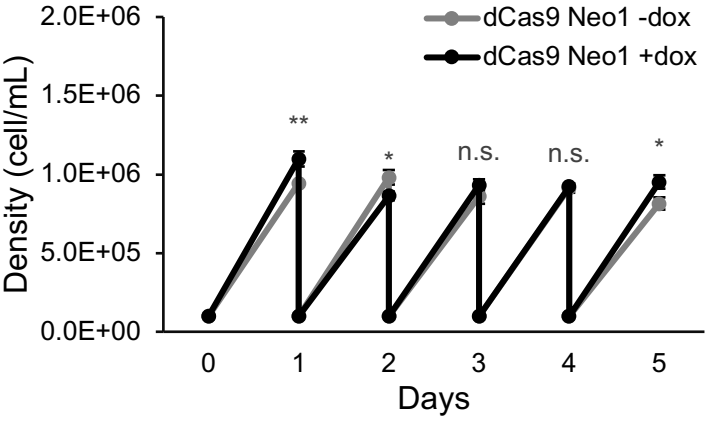
dCas9 Neo1 -dox
dCas9 Neo1 +dox
Density (cell/mL)
2.0E+06
1.5E+06
1.0E+06
5.0E+05
0.0E+00
**
*
n.s.
n.s.
*
0
1
2
3
4
5
Days

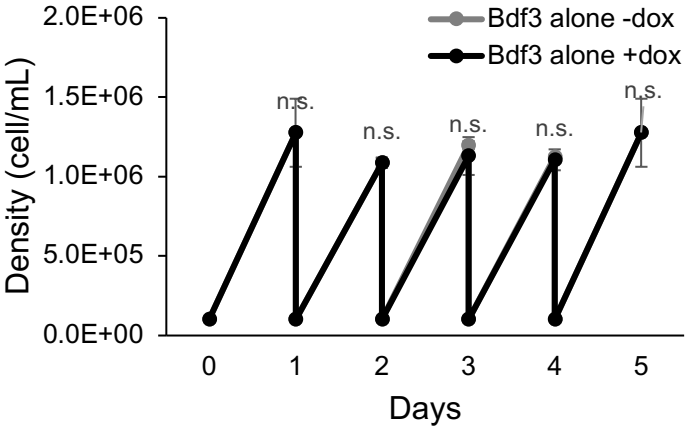
Bdf3 alone -dox
Bdf3 alone +dox
Density (cell/mL)
2.0E+06
1.5E+06
1.0E+06
5.0E+05
0.0E+00
n.s.
n.s.
n.s.
n.s.
n.s.
0
1
2
3
4
5
Days

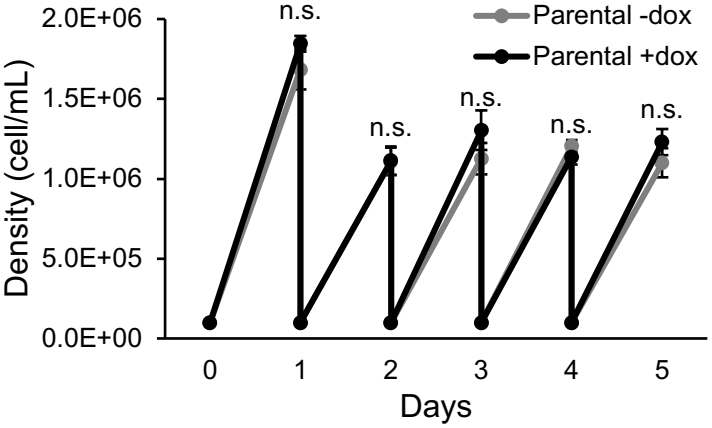
Parental -dox
Parental +dox
Density (cell/mL)
2.0E+06
1.5E+06
1.0E+06
5.0E+05
0.0E+00
n.s.
n.s.
n.s.
n.s.
n.s.
0
1
2
3
4
5
Days

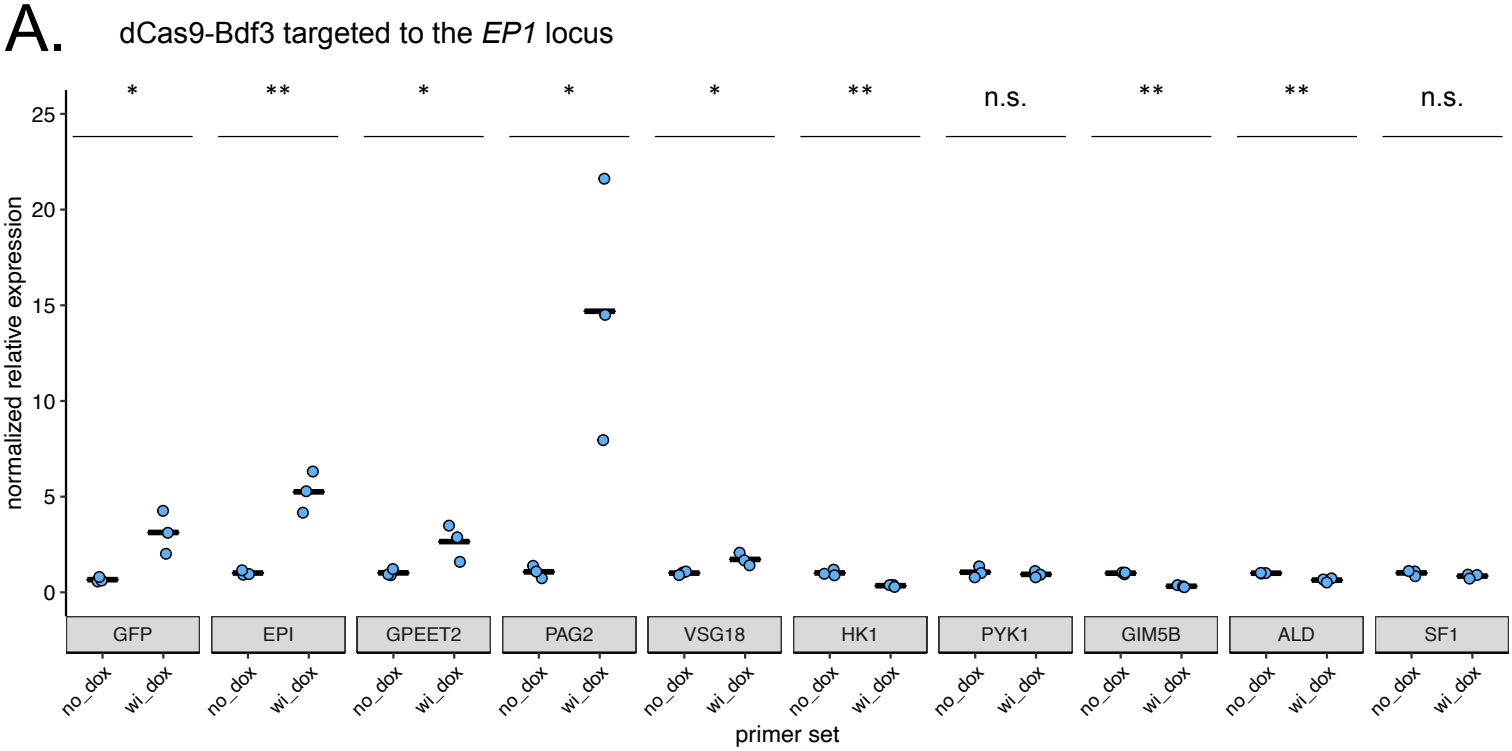
A.
dCas9-Bdf3 targeted to the *EP1* locus
*
**
*
*
*
**
n.s.
**
**
n.s.
normalized relative expression
25
20
15
10
5
0
GFP
EPI
GPEET2
PAG2
VSG18
HK1
PYK1
GIM5B
ALD
SF1
no_dox
wi_dox
primer set

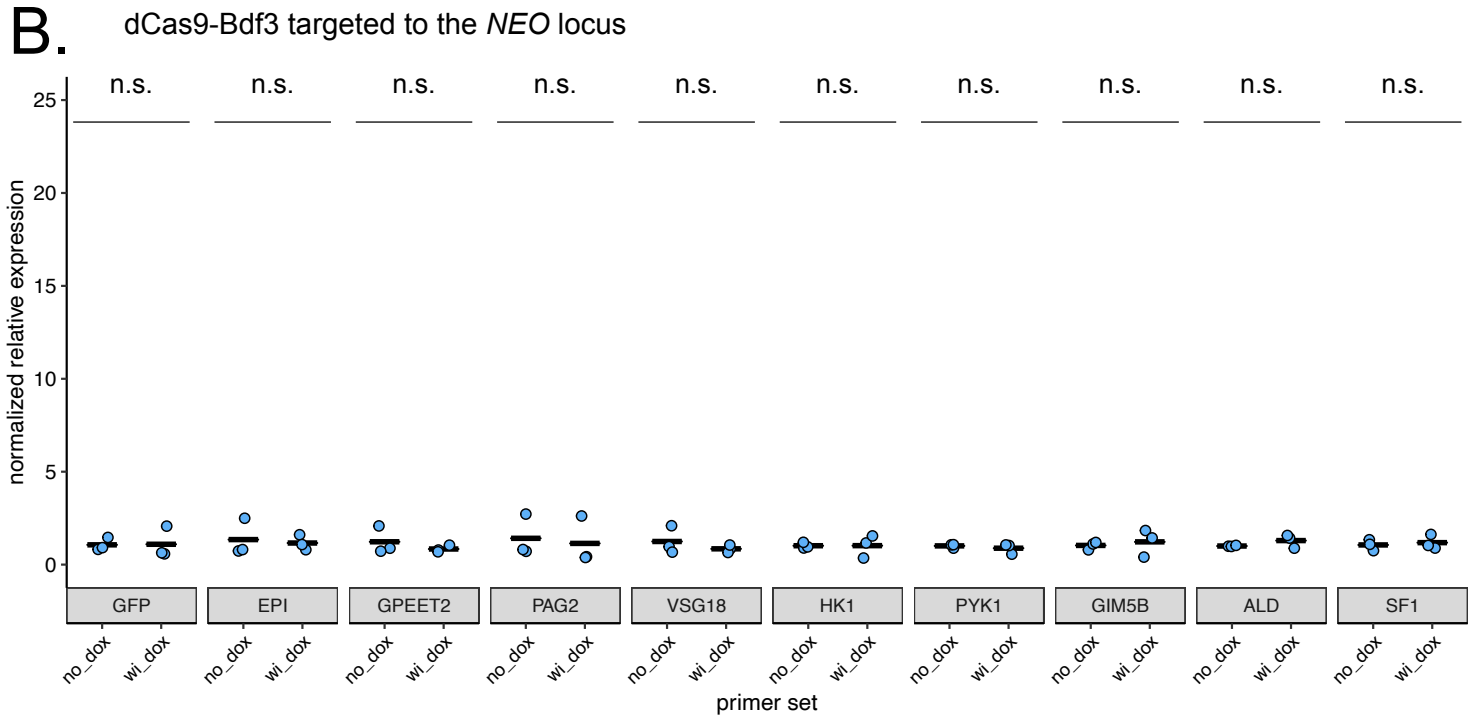
B.
dCas9-Bdf3 targeted to the *NEO* locus
n.s.
n.s.
n.s.
n.s.
n.s.
n.s.
n.s.
n.s.
n.s.
n.s.
normalized relative expression
25
20
15
10
5
0
GFP
EPI
GPEET2
PAG2
VSG18
HK1
PYK1
GIM5B
ALD
SF1
no_dox
wi_dox
primer set